Applied Catalysis B: Environmental 96 (2010) 198–207

Contents lists available at ScienceDirect

Applied Catalysis B: Environmental

journal homepage: www.elsevier.com/locate/apcatb

Investigation of coke formation on Ni-Mg-Al catalyst for hydrogen production from the catalytic steam pyrolysis-gasification of polypropylene

Chunfei Wu, Paul T. Williams*

Energy & Resources Research Institute, The University of Leeds, Leeds, LS2 9JT, UK

ARTICLE INFO

Article history:
Received 27 November 2009
Received in revised form 5 February 2010
Accepted 13 February 2010
Available online 20 February 2010

Keywords:
Polypropylene
Nickel
Coke
Gasification
Magnesium
Catalyst

ABSTRACT

Co-precipitated Ni-Mg-Al catalyst was prepared and investigated in relation to the production of hydrogen from the catalytic steam pyrolysis-gasification of polypropylene using a two-stage reaction system. Coke formation on the Ni-Mg-Al catalyst was investigated by using temperature-programmed oxidation (TPO), X-ray diffraction (XRD), scanning electron microscopy (SEM)/energy dispersive X-ray spectroscopy (EDXS), transmission electron microscopy (TEM) and focused ion beam (FIB)/scanning electron microscopy (SEM). The coke formation mechanism on the Ni-Mg-Al catalyst is proposed. It is suggested that the Ni-Mg-Al catalyst is initially reduced during the gasification process, the reactions of decomposition/reforming of hydrocarbons gases occur on the surface and inside the catalyst; this resulted in partial fragmentation of the catalyst into small particles. Layered carbons, perhaps containing monoatomic carbon, metal carbides, etc., are suggested to be a transition layer for the formation of filamentous carbons. The addition of Mg into the Ni-Al catalyst was found to increase the catalytic activity and the physical stability of catalyst. In addition, increasing the calcination temperature from 750 to 850 °C reduced the surface area of the fresh Ni-Mg-Al catalyst, increased the NiO crystal size, and resulted in a decrease of catalytic activity in the pyrolysis-gasification of polypropylene; however, a more stable catalyst was obtained with higher calcination temperature.

1. Introduction

Nickel-based catalysts have been extensively used in the gasification process of many different feedstocks [1–3]. Although noble metals such as Ru and Rh are reported to be more effective than nickel-based catalysts, they are not commonly used in industry because of their high cost [4]. In this paper, we have investigated the use of a nickel-based catalyst applied in the production of hydrogen from the catalytic steam pyrolysis-gasification of plastics; this process has shown potential as a viable alternative route for hydrogen production and additionally a promising way to manage waste plastics [5–8].

Coke formation on the surface of nickel catalysts is one of the major problems in catalytic reforming reactions because it results in deactivation of the catalyst [9–11]. Three types of carbon have been reported by Sehested [12]: pyrolytic, encapsulating and whisker carbon. Most of the pyrolytic carbons are suggested to be formed by carbonization of hydrocarbons upstream of the catalytic reactions. Certain consideration should be given to the design of the reaction system or introduction of the oxidation agent to gasify the pyrolytic carbons before they aggregate to block the reaction tube or before they enter the catalytic zone and deactivating the catalyst. Hayashi et al. [13] presented a concept to separate the oxidation of coke (pyrolytic) from the catalytic steam gasification reactions. Encapsulating and whisker carbon may be formed on the catalyst during reforming of heavy hydrocarbon feeds with a high content of aromatic compounds [12]. It is known that the encapsulating carbons are mostly responsible for the deactivation of catalysts, although the filamentous carbons might cause a pressure drop and reactor blockage.

The coke deposition on the catalyst may be influenced by process conditions such as the preparation of the catalyst or the reaction temperature etc. It has been reported that the size of nickel crystallites of nickel-based catalysts determines the formation rate of carbon deposition [14], and the metal support interactions may also have an important role in coke formation during the gasification of hydrocarbons [15–17]. In addition, the coke formation may also be influenced by the type of feedstock and the reaction conditions (steam injection, gasification temperature and catalyst amount, etc.).

In this paper, a possible formation mechanism of coke formation on a Ni-Mg-Al catalyst has been proposed during the catalytic steam pyrolysis-gasification of polypropylene, while the influences of other parameters such as reaction conditions and type of feed-

* Corresponding author. Tel.: +44 1133432504.
E-mail address: p.t.williams@leeds.ac.uk (P.T. Williams).

0926-3373/$ – see front matter © 2010 Elsevier B.V. All rights reserved.
doi:10.1016/j.apcatb.2010.02.022

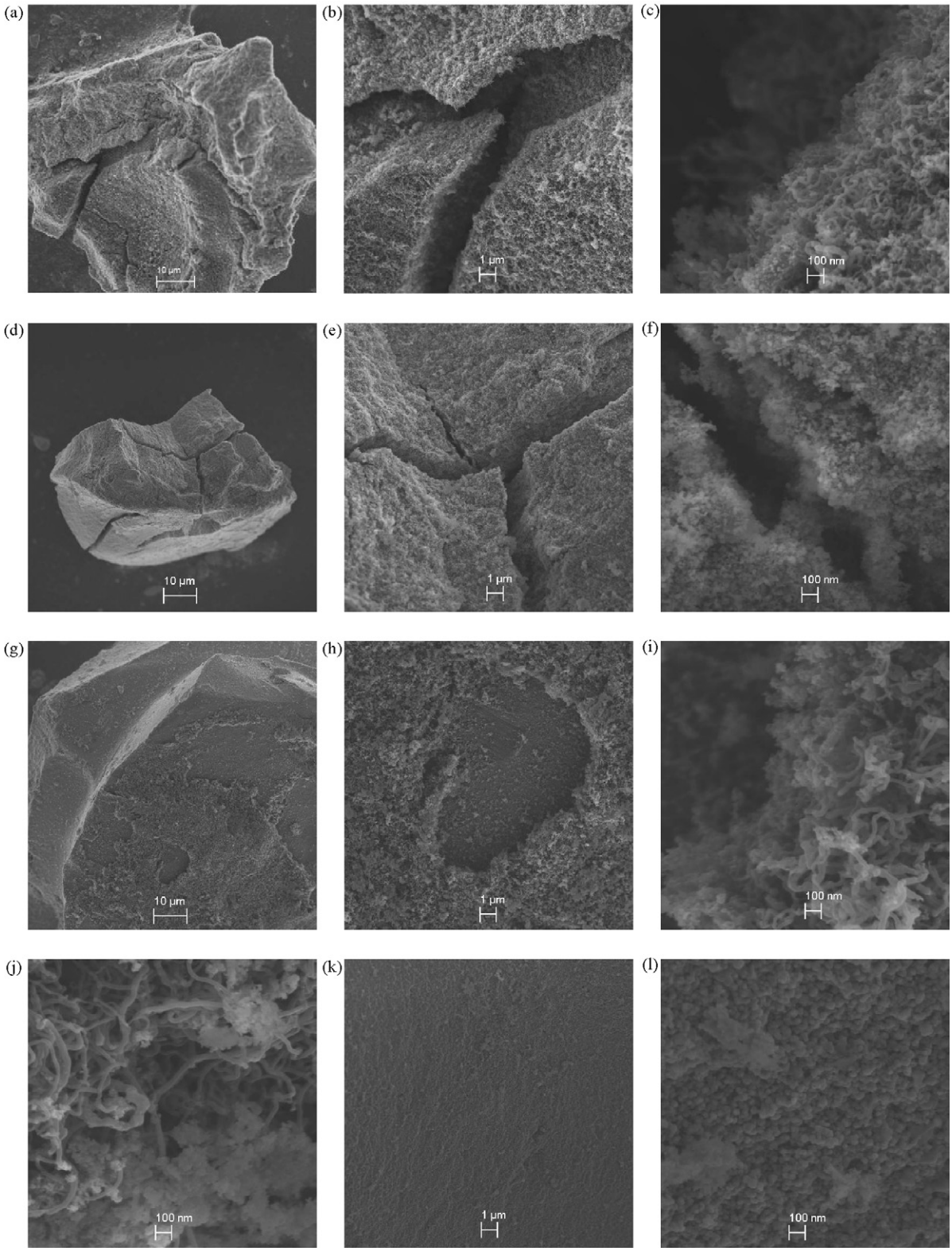

Fig. 1. The SEM results for the reacted Ni-Mg-Al catalyst.

stock were not considered. The influences of Mg addition and calcination temperature on coke formation were also investigated.

2. Experimental

2.1. Materials

Polypropylene was obtained as 2 mm virgin polymer pellets provided by BP Chemicals, UK. The temperature-programmed degradation of feedstock (polypropylene) in N_2 shows that the polymer started to be decomposed at about 420 °C and completed at 510 °C; in addition, almost no residue was collected after the experiment.

Ni-Al and Ni-Mg-Al catalysts were prepared using the rising pH technique according to the method reported by Garcia et al. [18]. The precipitant 1 M $NH_4(OH)$ was added to 200 ml of an aqueous solution containing $Ni(NO_3)\cdot 6H_2O$ and $Al(NO_3)_3\cdot 9H_2O$ with or without the addition of $Mg(NO_3)_2\cdot 6H_2O$. The precipitation was carried out at 40 °C with moderate stirring until the final pH (7.9 for Ni-Al catalyst, 8.3 for Ni-Mg-Al catalyst) was obtained. The precipitates were filtered and washed with water (40 °C), followed by drying at 105 °C overnight, and then were calcined at 750 or 850 °C for 3 h. The Ni-Al catalyst with a molar ratio of 1:2 was prepared. Ni-Mg-Al catalysts with molar ratio of 1:1:1 was prepared. In this paper, Ni-Al catalyst is presented as Ni-Al; Ni-Mg-Al catalyst calcined at 750 °C is presented as Ni-Mg-Al; Ni-Mg-Al catalyst calcined at 850 °C is presented as Ni-Mg-Al (1:1:1, 850). The actual molar ratio of Ni-Al, Ni-Mg-Al and Ni-Mg-Al (1:1:1, 850) catalysts were calculated from the analysis of energy dispersive X-ray spectroscopy and were 1:1.8, 1:0.6:1 and 1:0.5:1, respectively.

All the catalysts used were crushed and sieved to granules with a size range between 0.065 and 0.212 mm. In addition, all the catalysts were not reduced by H_2.

2.2. Reaction system

The two-stage, pyrolysis-gasification reaction system consisted of a first stage pyrolysis reactor heated by a tube furnace and a second gasification reactor separately heated by a second tube furnace. Both furnaces were thermally controlled separately. The polypropylene was placed in the first reactor where pyrolysis of the polypropylene occurred. The evolved pyrolysis gases passed through to the second gasification reactor containing the catalyst and where steam was introduced and the reforming reactions were carried out. During the experiment, 1 g of polypropylene and 0.5 g of catalyst were used. The second stage gasification reactor was heated upto 800 °C, and then the first stage pyrolysis reactor was started to be heated to 500 °C with a heating rate of 40 °C min^{-1}. The water for steam production was introduced via a syringe pump with a flow rate of 4.74 g h^{-1} when the temperature of the first reactor had reached 400 °C. The reaction time was 30 min after the injection of water, and a further 20 min were required to ensure all the product gases were collected.

The derived gases from the catalytic steam pyrolysis-gasification of polypropylene were condensed by two condensers and the liquids were collected. The non-condensed gases were collect in a Tedlar™ gas bag and analysed by packed column gas chromatography. C_1–C_4 hydrocarbons were analysed using a Varian 3380 gas chromatograph with a flame ionisation detector, with a 80–100 mesh Hysep column and nitrogen carrier gas. Permanent gases (H_2, CO, O_2, N_2 and CO_2) were analysed by a second Varian 3380 GC with two separate columns. Hydrogen, oxygen, carbon monoxide and nitrogen were analysed on a 60–80 mesh molecular sieve column with argon carrier gas, whilst carbon dioxide was analysed on a Hysep 80–100 mesh column with argon carrier gas.

2.3. Analysis methods catalysts

The temperature-programmed oxidation (TPO) of the reacted catalysts was carried out using a Stanton-Redcroft thermogravimetric analyser (TGA) to determine the properties of the coked carbons deposited on the reacted catalysts. The differential thermogravimetry (DTG) results from the TPO experiments were also examined. About 100 mg of the reacted catalyst was heated in the TGA in an atmosphere of air at 15 °C min^{-1} to a final temperature of 800 °C, with a dwell time of 10 min.

The reacted catalysts were also analysed by X-ray diffraction (XRD). The analysis was carried out with a Philips PW 1050 Goniometer using a PW 1730 with a CuKα radiation X-ray tube. The sample was ground to less than 75 μm size and loaded into the 20 mm aperture of an aluminium sample holder. The data was collected by Hiltonbrooks' HBX data acquisition software. The phase identification was obtained using GBC Scientific Equipment Ltd. TRACES software using the ICDD PDF2 (International Centre for Diffraction Data Powder Diffraction Files) database.

Several advanced electron microscopy systems were used to examine and characterise the reacted catalysts. A high resolution scanning electron microscopy (SEM, LEO 1530) coupled to an energy dispersive X-ray spectroscopy (EDXS) was used to characterise and examine the characteristics of the carbon deposited on the coked catalysts. Transmission electron microscopy (TEM) (Philips CM200) coupled with EDXS was used to determine the characteristics of the reacted Ni-Al (1:1) catalyst. For the TEM analysis, the sample was ground, dispersed with acetone, and then deposited on a Cu grid covered with a perforated carbon membrane. A FEI Nova 200 Nanolab Dualbeam Focuses Ion Beam (FIB)/scanning electron microscope (SEM) coupled to an energy dispersive X-ray spectroscopy (EDXS) was also used to analyse the cross-section of the reacted catalyst.

3. Results and discussion

3.1. Coke formation on the nickel catalyst

In this paper, a nickel-based catalyst has been applied to the catalytic steam pyrolysis-gasification of polypropylene. How the coke formed on the surface of the Ni-Mg-Al catalyst during the steam pyrolysis-gasification of polypropylene will be discussed.

It has been reported that the NiO phase could be reduced to Ni by the reducing gases such as H_2 and CO produced during the gasification process [19]. Therefore, the non-reduced fresh Ni-Mg-Al catalyst prepared in this paper might be reduced first to generate

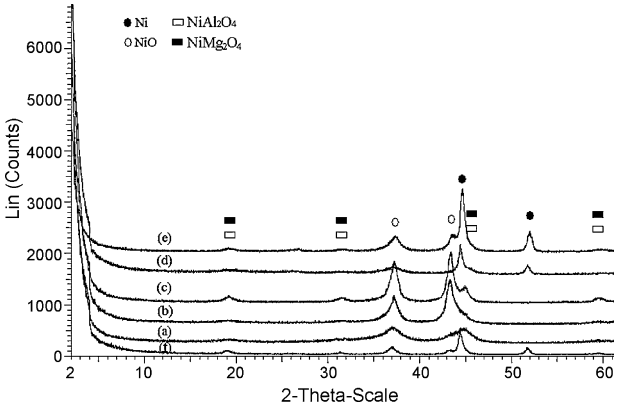

Fig. 2. XRD analysis from different nickel catalysts: (a) fresh Ni-Al; (b) fresh Ni-Mg-Al; (c) fresh Ni-Mg-Al (1:1:1, 850); (d) reacted Ni-Al; (e) reacted Ni-Mg-Al; (f) reacted Ni-Mg-Al (1:1:1, 850).

a Ni phase, which is known to be an active site for the catalytic reactions.

3.1.1. SEM analysis of reacted catalyst

From the SEM analysis to the reacted Ni-Mg-Al catalyst (Fig. 1), it seems that some of the catalyst particles were cracked and fragmented into small particles after the steam reforming process. Filamentous carbons were observed on the cracked surface of the reacted Ni-Mg-Al (1:1:1) catalyst (Fig. 1(a–c)). However, not all the catalyst particles with surface breakup were covered with the filamentous carbons after the steam reforming process. Fig. 1(d–f) shows that the catalyst particle was cracked, and a layer of carbon seems to be deposited on the surface of catalyst. This layer of carbon might be assigned to layered carbons. The non-cracked catalyst after the steam gasification of hydrocarbons derived from pyrolysis of plastics is also shown in Fig. 1(g–i). From Fig. 1(g–i), both filamentous carbons and layer carbons were observed. Only parts of the surface of the catalyst were covered after the reaction time which was about 30 min in this work. Filamentous carbons appeared to be formed on the top of the layered carbons as indicated in Fig. 1(i) and (j). The comparatively cleaner surface for the reacted Ni-Mg-Al (1:1:1) catalyst is also shown in Fig. 1(k) and (l). A few layered carbons were found on the surface of the catalyst particle shown in Fig. 1(k) and (l). Numerous small particles were observed on the particles surface (Fig. 1(l)). These small particles might be Ni metal reduced from the original catalyst.

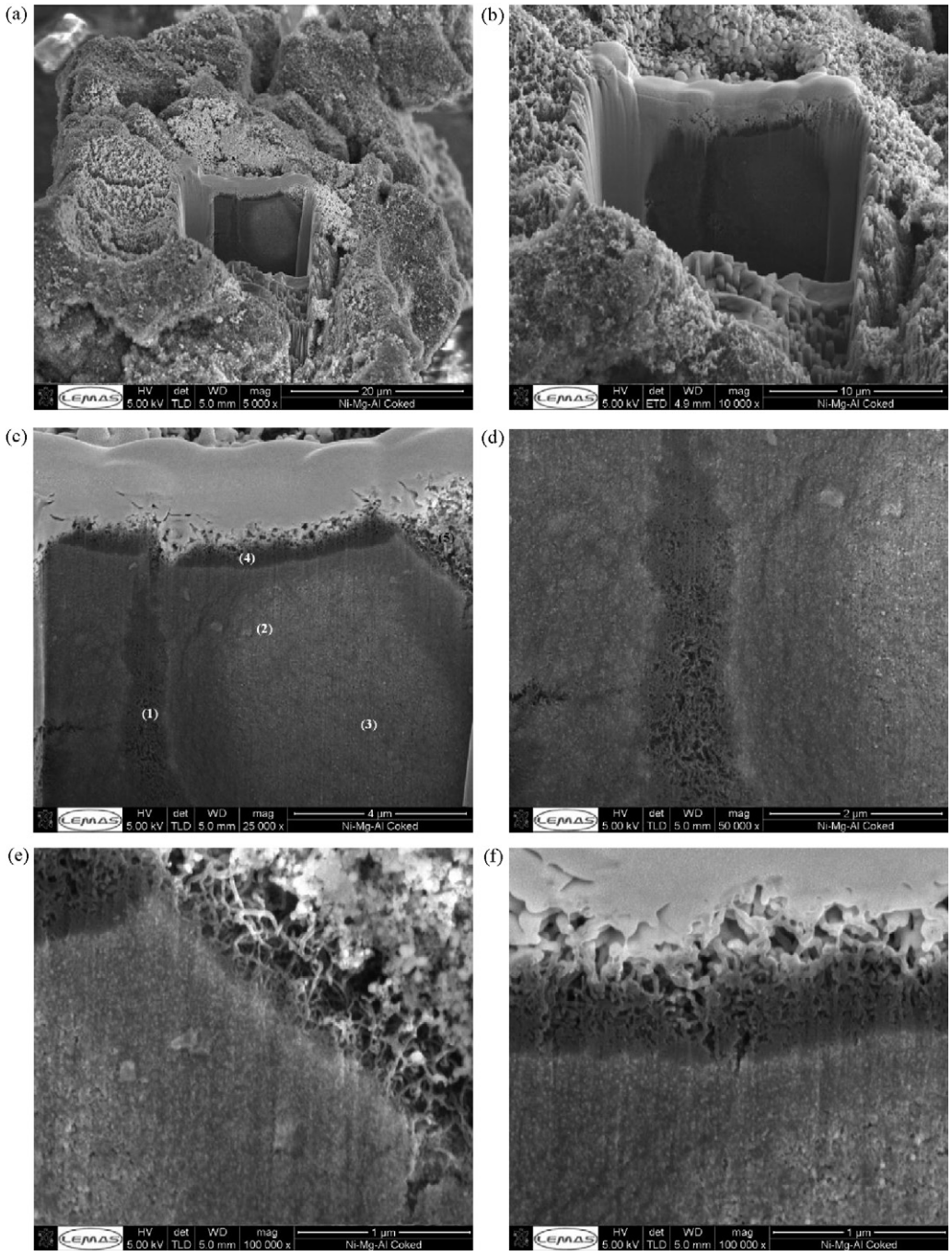

Fig. 3. Cross-section images of the reacted Ni-Mg-Al catalyst: (a), (b) and (c) are in different magnification; (d), (e) and (f) are the area magnification of (c).

3.1.2. XRD analysis

The XRD analysis for the fresh and reacted catalysts is shown in Fig. 2. NiO and spinel phases were observed for the fresh catalyst. After the steam reforming reaction, a Ni phase was obtained for all the catalysts (Fig. 2).

3.1.3. FIB/SEM analysis

More details about the reacted Ni-Mg-Al catalyst were obtained by the analysis of a cross-section of the catalyst using FIB/SEM technology. The images of cross-section of the reacted catalyst are shown in Fig. 3. The EDXS results from different spot analyses of the catalyst shown in Fig. 3(c) are also presented in Fig. 4. It has to be pointed out that the top layer of the cross-section is coated platinum used to protect the sample during the cutting of the catalyst. Two distinct layers were observed on the top of the catalyst observed from Fig. 3. It can be suggested from the above discussion (SEM) that one layer of layered carbons was formed on the top of the catalyst, and then a layer of filamentous carbon was produced on top of the layered carbons. However, for the layered carbons, all the elements (Ni, Mg and Al) from the catalysts were found from the EDXS results (Fig. 4(4)). Therefore, the layered carbons mentioned in this paper might be a loose structure of catalyst mixed with monoatomic carbons or carbides. In addition, filamentous carbons are not distinctively separated from the layered carbons. Since, the roots of filamentous carbons seemed to be inside the layered carbons.

From Fig. 4(2) and (3), carbon content was also detected inside the catalyst; and more carbon content was found when the detected spot was close to the surface of catalyst. It is suggested that some gases might permeate into the catalyst and decompose to generate carbon inside the catalyst during the gasification process. The reaction inside of the catalyst might be an initial force to crack the catalyst into small particle fractions.

Filamentous carbons were observed in the cracked formed in the catalyst (Fig. 3(d) and Fig. 4(1)). From Fig. 4(1), only C, O and Ni contents were obtained. It is suggested that filamentous carbons were formed with the participation of Ni. Ni particles were found on the top of filamentous carbons as has been extensively reported [5,20,21].

3.1.4. Coke formation mechanism for Ni-Mg-Al catalyst during pyrolysis-gasification of polypropylene

From the above observation, we suggest that during the steam reforming of hydrocarbons derived from the pyrolysis of polypropylene, catalysts might be reduced to generate a Ni phase as shown in Fig. 1(l). At the same time or after catalyst reduction, decomposition/reforming of hydrocarbons occurred on the surface of the catalyst as well as inside of the catalyst. The catalyst particles might be cracked into small particles due to the reactions occurring inside the catalyst. A surface breakup was observed by Louis et al. [22], while the growth of carbon nanofibers was investigated over a nickel catalyst supported on graphite microfibers. Louis et al. [22] suggested that a Ni-rich carbon zone was formed initially by carbon saturation on Ni particles during the catalytic decomposition of C_2H_6, and then the release of dissolved carbon caused the lift-off of the Ni-rich carbon particles and resulted in surface breakup.

With the further decomposition of hydrocarbons derived from pyrolysis of polypropylene, formation of non-stoichiometric metal carbides [23,24] or reactive carbons [25,26] occurs initially. The formation of metal carbides or reactive carbons might be assigned to the layered carbons, and the layered carbons are suggested to be a transition layer to the formation of filamentous carbons. These initially formed carbonaceous materials might be further dissolved and diffused into the nickel particles; this process was regarded to be essential to the growth of carbon whiskers [27,28]. Natesakhawat et al. [29] also suggested that the carbonaceous species from the decomposition of propane further dissolve and diffuse through the nickel particles, and are accompanied by precipitation at the rear of the nickel particle with formation of a carbon filament. Chinthaginjala et al. [30] reported that large amounts of

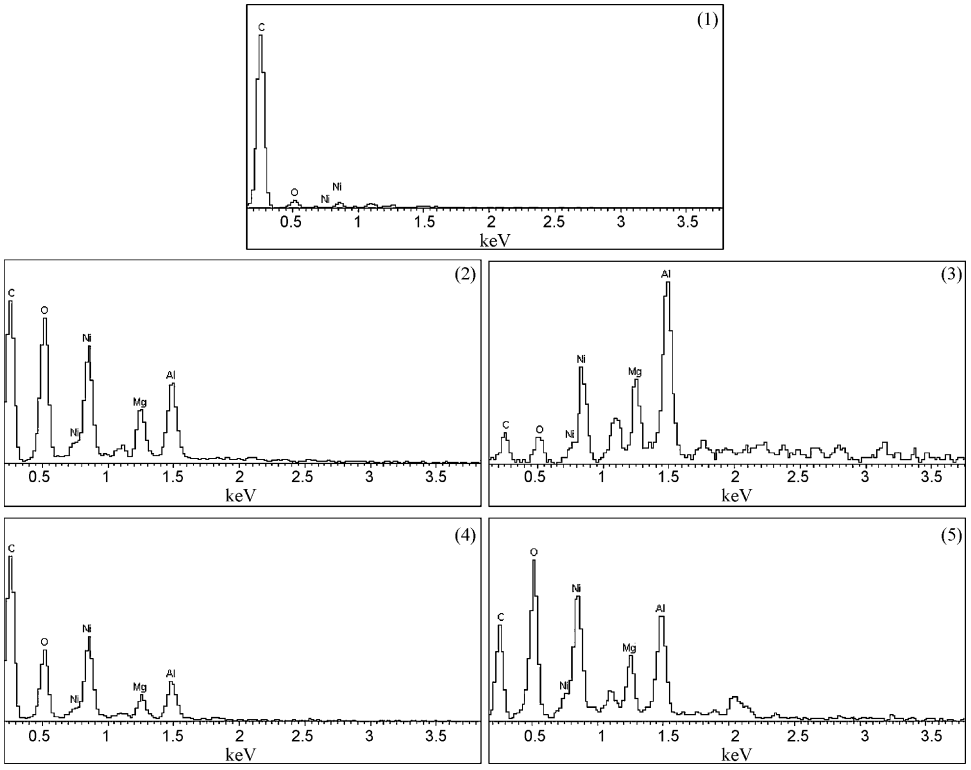

Fig. 4. EDXS results from different pots in Fig. 3 (c).

filamentous carbons were produced after the initial formation of layered carbons and the filamentous carbons are formed on the top of layered carbons.

It is suggested that not all of the initially formed carbonaceous material dissolved and converted into the filamentous carbons, some might remain on the surface of the catalyst and encapsulate the nickel particles [27,28]. It has been reported that the layered carbons (encapsulating) are easier to be gasified than the less reactive filamentous carbon [31,32].

Therefore, we propose a model for coke formation on the Ni-Mg-Al catalyst during the catalytic steam pyrolysis-gasification of polypropylene. At first, the pyrolysed gases such as H_2, CmHn, etc. derived from the first stage pyrolysis reactor passed through the second stage catalyst bed, where the non-pre-reduced catalyst might be reduced to generate Ni particles. Some carbons might be generated on the surface or inside of the catalyst, results in a cracking of the fresh catalyst. The produced carbonaceous materials might be then dissolved into the Ni particles and a reactive type of carbon (layered carbons) or metal carbides were formed. With the further process of gasification, filamentous carbons (less reactive) might be developed on the top of layered carbons. During the formation of carbons, it has to be pointed out the gasification of carbons also occurs. Therefore, the total deposited carbons would depend on the balance of the carbon formation rate and the carbon gasification rate.

3.2. The influence of Mg addition to Ni-Al catalyst on the coke formation

The experimental results from the pyrolysis-gasification of polypropylene with Ni-Al and Ni-Mg-Al catalyst are shown in Table 1. It should be pointed out that the detailed experimental results for the catalytic steam pyrolysis-gasification of polypropylene have already been presented in our previous work [5]. In this paper, the results of pyrolysis-gasification are used to discuss the coke formation.

From the XRD analysis to the fresh and reacted catalyst (Fig. 2(a) and (b)), it seems that the NiO phase in the Ni-Mg-Al catalyst shows higher peak intensity than the one in the Ni-Al catalyst. More NiO phase in the Ni-Mg-Al catalyst should result in more Ni phase after the gasification reaction; this is confirmed from the XRD results (Fig. 2(d) and (f)). Furthermore, the higher concentration of Ni in the reacted Ni-Mg-Al catalyst compared with the Ni-Al catalyst, was also obtained from the DTG-TPO results (Fig. 5) [5]. The weight ratio in Fig. 5 was presented as the weight of sample at each TPO temperature divided by the initial weight of sample.

Table 1
Results of catalytic steam pyrolysis-gasification of polypropylene [5].

	Catalyst		
	Ni-Al	Ni-Mg-Al	Ni-Mg-Al
Molar ratio	1:2	1:1:1	1:1:1
Calcination temperature (°C)	750	750	850
Gas yield (wt.%)	96.0	99.1	91.9
Oil yield (wt.%)	0.0	0.0	0
Solid yield (wt.%)	2.8	0.5	2.8
Mass balance (wt.%)	98.8	99.6	94.7
Gas composition (vol.%)			
CO	25.7	27.7	28.2
H_2	64.0	62.2	61.8
CO_2	6.4	7.0	7.0
CH_4	3.3	2.9	3.0
C_2–C_4	0.6	0.1	0.02
Reacted water (g)	1.21	1.40	1.13
Potential H_2 production (wt.%)	53.1	57.1	46.4

During the DTG-TPO experiment, the increasing peak at around 350 °C is suggested to be due to the oxidation of Ni; and the higher oxidation peak of Ni for the Ni-Mg-Al catalyst was obtained from the DTG-TPO results [5]. Therefore, the higher catalytic activity of the Ni-Mg-Al catalyst might be due to its higher content of Ni metal. The enhanced performance of Mg addition to the Ni-Al catalyst was also obtained for the pyrolysis-gasification of polypropylene. For example, the gas yield and hydrogen production were increased with the addition of Mg to the Ni-Al catalyst. The water consumed in the pyrolysis-gasification process was also increased from 1.21 to 1.40 g by introducing Mg metal into the catalyst (Table 1).

The addition of Mg into the Ni-Al catalyst seems to reduce the amount of coke deposited on the nickel catalyst. From our previous

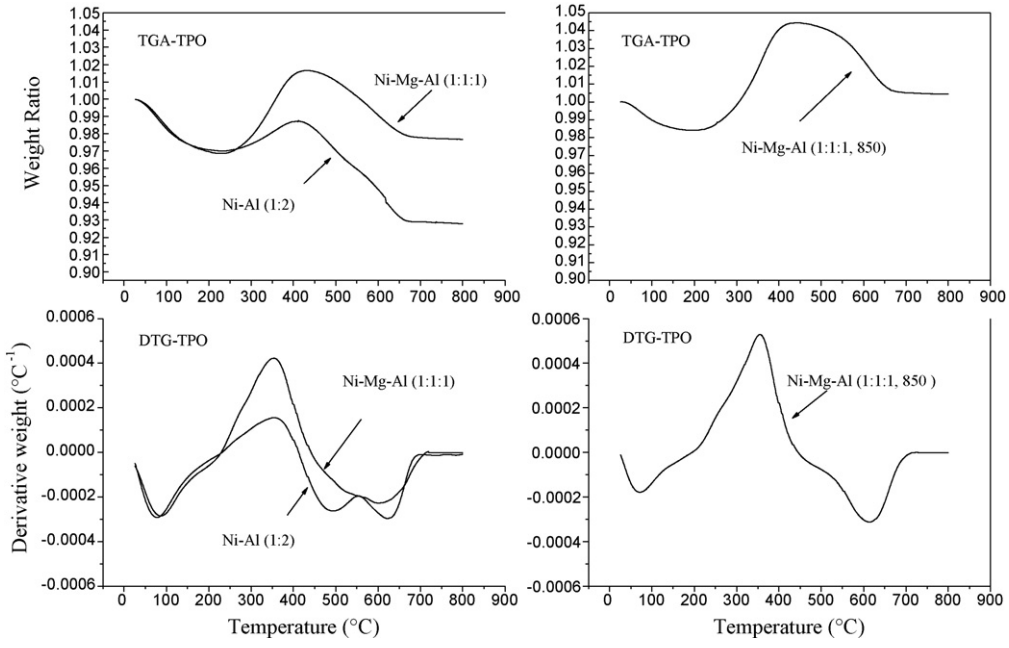

Fig. 5. TGA-TPO and DTG-TPO of reacted nickel catalyst [5].

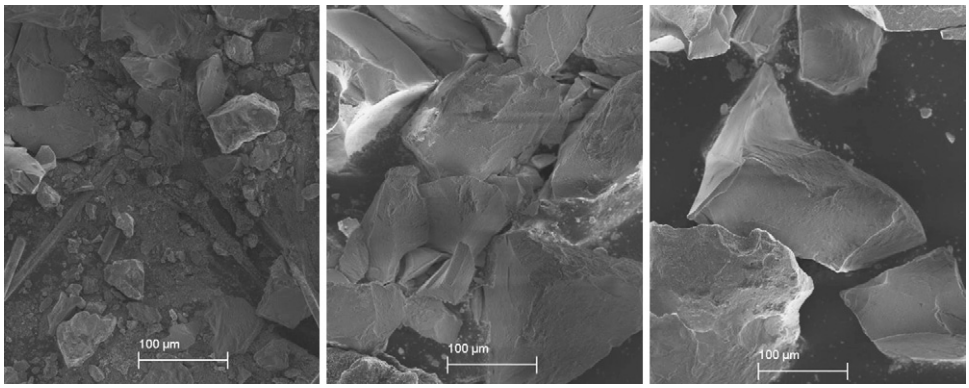

Fig. 6. SEM results of the reacted catalyst; (a) Ni-Al; (b) Ni-Mg-Al; (c) Ni-Mg-Al (1:1:1, 850).

work concerning TPO experiments [5], the amount of coke formed was reduced from around 5.9 to 3.9 wt.% when the catalyst was changed from Ni-Al to Ni-Mg-Al. It has been suggested that the layered carbons have a lower oxidation temperature than the filamentous carbons [33]. From the TPO experiments (Fig. 5) [5], the oxidation peak for the layered carbon disappeared for the reacted Ni-Mg-Al catalyst. It is suggested that the reduced carbon amount deposited on the Ni-Mg-Al catalyst compared to Ni-Al might be due to the lower content of layered carbons. The addition of Mg into the Ni-Al catalyst might improve the gasification rate of carbons especially the more reactive carbons, the layered carbons. The removal of the layered carbons might reduce the encapsulation of Ni particles, avoid the deactivation of catalyst and finally improve the catalytic activity of catalyst.

The addition of Mg into the Ni-Al catalyst might increase the mechanical stability of the catalyst. Fig. 6 shows the SEM results, with low magnification, of the reacted catalyst. From Fig. 6, it seems that more fragmentation of the catalyst occurred producing

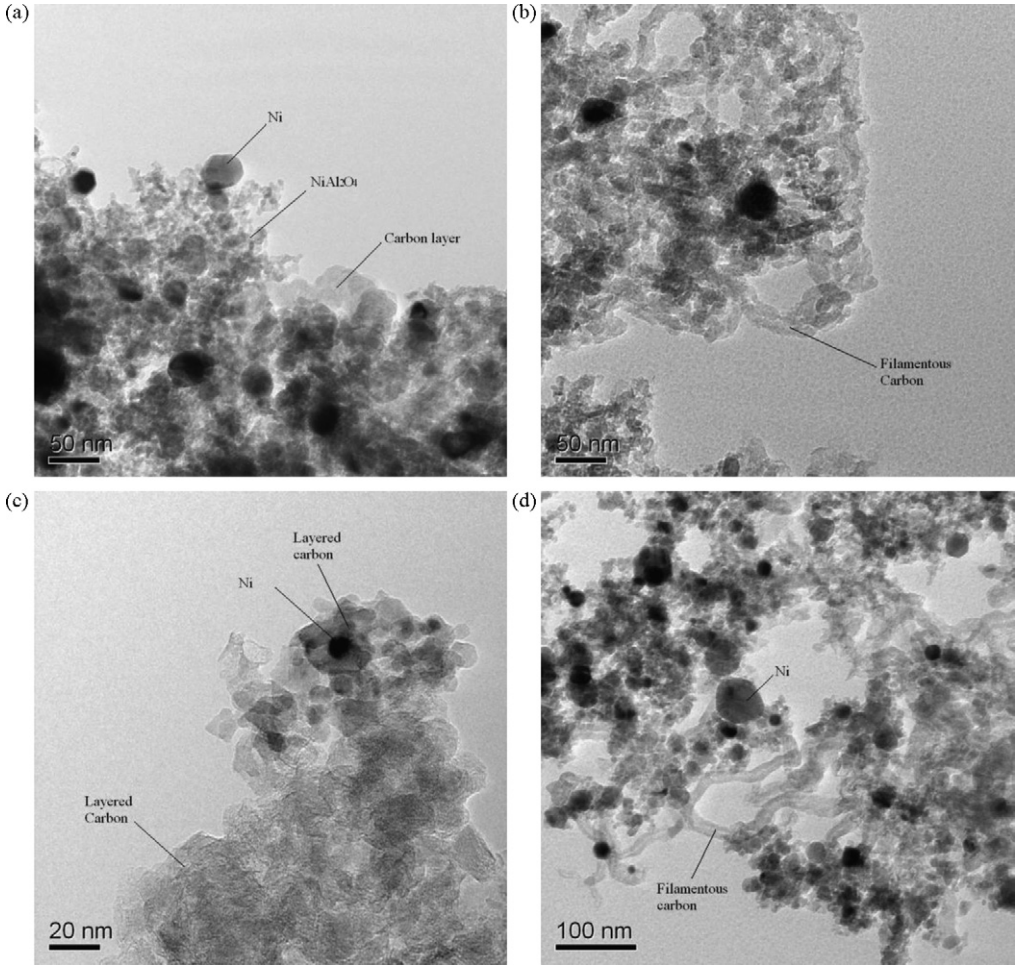

Fig. 7. TEM results of the reacted catalyst: (a–b) Ni-Al; (c–d) Ni-Mg-Al.

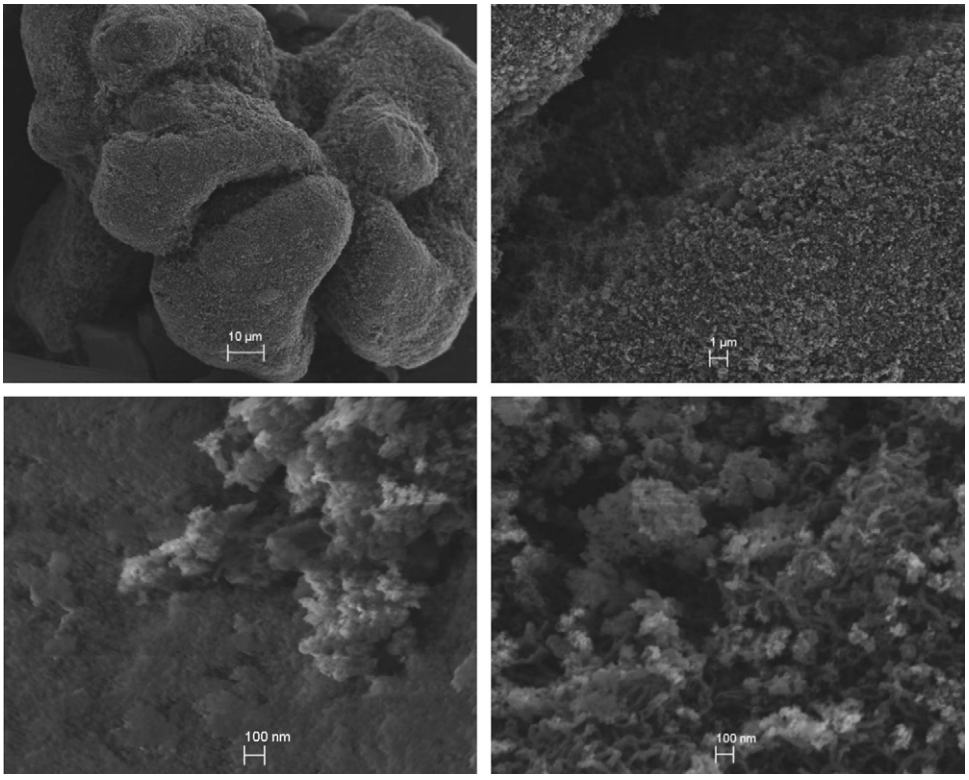

Fig. 8. SEM results for the reacted Ni-Mg-Al (1:1:1, 850) catalyst.

powder for the reacted Ni-Al catalyst, while the Ni-Mg-Al catalyst shows a comparative stability after the catalytic steam pyrolysis-gasification reactions. The addition of Mg has been reported to be able to replace nickel in the crystal structure and improve the physical strength of the catalyst [34,35]. The increased physical strength of the Ni-Mg-Al catalyst might have a positive effect to reduce the coke formation on the surface of the catalyst.

The TEM results of the reacted Ni-Al and Ni-Mg-Al catalyst are shown in Fig. 7. Ni particles were observed with various sizes for both reacted Ni-Al and Ni-Mg-Al catalysts. Carbon layers and the filamentous carbons were also observed from the TEM analysis. It appeared that there was no obvious relation between the diameter of the filamentous carbons and the Ni particle size (Fig. 7). However, from Fig. 7(d), diameters of filamentous carbons were similar to the sizes of adjacent Ni particles. The comparatively larger Ni particles, observed in Fig. 7(d), might be formed by aggregation of small Ni particles during the non-uniform cracking of hydrocarbons.

3.3. *The influence of calcination temperature on the coke formation*

Calcination temperature plays an important role in catalyst performance. Too high calcination temperature was suggested to increase the reduction temperature of the catalyst and reduce the catalytic activity, whereas a low calcination temperature might reduce the stability of the catalyst and results in quick deactivation [36–38]. In this section, the calcination temperature for the Ni-Mg-Al catalyst was investigated in terms of its influence on coke formation on the surface of the catalyst.

Two calcination temperatures of 750 and 850 °C were investigated for the steam catalytic pyrolysis-gasification of polypropylene. From the BET surface area analysis, the BET surface area of the fresh catalyst was reduced from 99 to 74 $m^2 g^{-1}$ [5]. From the XRD analysis (Fig. 2), we obtained that the NiO crystal size increased from 81.4 to 91.6 Å with the increase of calcination temperature. The amount of the reducible NiO phases might be reduced by the increase of calcination temperature. From Fig. 2, the intensity of the NiO phase for the Ni-Mg-Al catalyst calcined at 750 °C was higher than the one calcined at 850 °C. In addition, the generated Ni phase in the reacted catalyst calcined at 750 °C was higher than the one calcined at 850 °C.

From Table 1, it is indicated that the gas yield and hydrogen production was reduced with the increase of calcination temperature, and the amount of reacted water during the gasification process was also reduced. It is suggested that the catalyst activity of Ni-Mg-Al was reduced with the increase of calcination temperature from 750 to 850 °C. The reduced catalytic activity of Ni-Mg-Al (1:1:1, 850) might be due to the lower amount of reduced Ni particles compared to the catalyst calcined at 750 °C.

The SEM results for the reacted Ni-Mg-Al (1:1:1, 850) catalyst are shown in Fig. 8. As shown in Fig. 8, it seems that the coke formation model we proposed above is suitable for the coke formation on the Ni-Mg-Al (1:1:1, 850) catalyst. Both layered and filamentous carbons were observed from the SEM analysis (Fig. 8). The total amount of coke formed on the catalyst calculated from the TGA-TPO experiment (Fig. 5) indicates that the amount of coke deposited was slightly decreased with the increasing calcination temperature for the Ni-Mg-Al catalyst. From the TEM analysis of the reacted Ni-Mg-Al (1:1:1, 850) catalyst (Fig. 9), it is difficult to find the filamentous carbons. This might be due to the preparation of the sample for the TEM analysis, or due to the lower amount of filamentous carbon deposited on the Ni-Mg-Al (1:1:1, 850) catalyst. From the DTG-TPO experiment (Fig. 5), the oxidation peak for the filamentous carbons seems to be moved from around 605 to 615 °C, and the oxidation peak becomes narrower when the catalyst was changed from Ni-Mg-Al to Ni-Mg-Al (1:1:1, 850). Therefore, more uniform filamentous carbons might be generated for the Ni-Mg-Al (1:1:1, 850) catalyst.

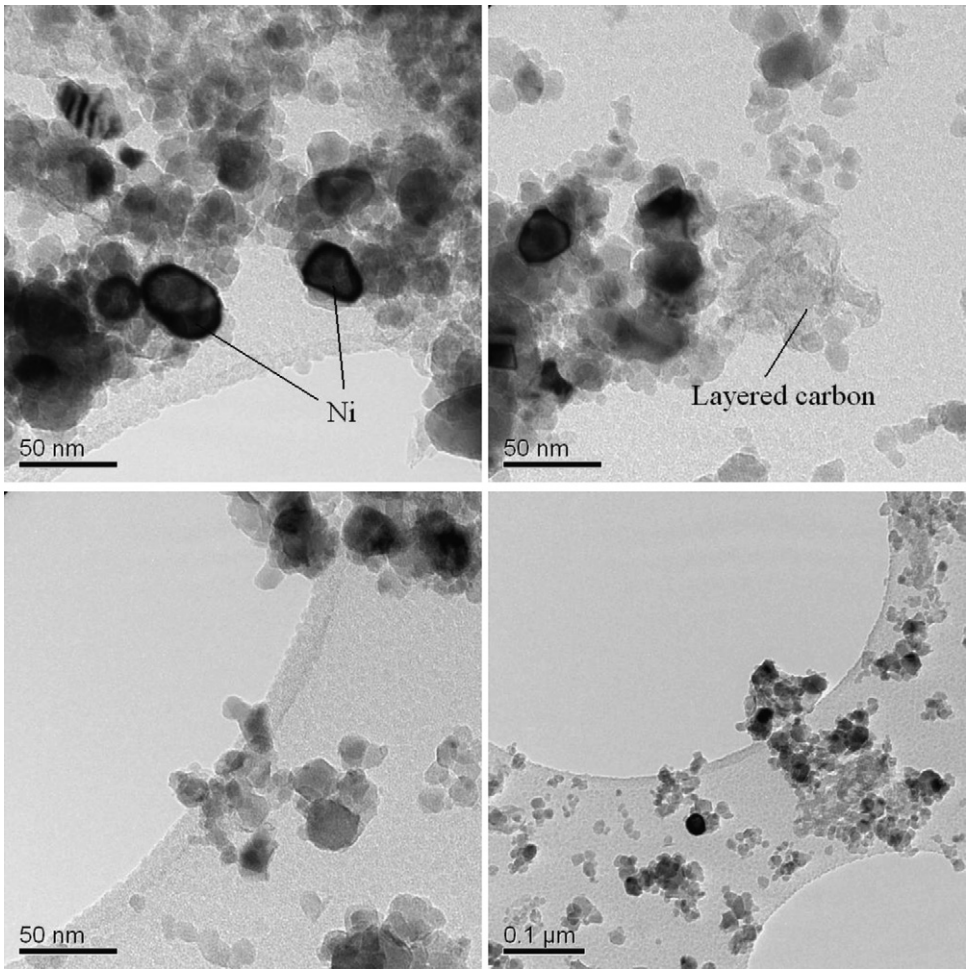

Fig. 9. TEM results of the reacted Ni-Mg-Al (1:1:1, 850) catalyst.

4. Conclusions

In this paper, a co-precipitated Ni-Mg-Al catalyst was prepared and tested for the catalytic steam pyrolysis-gasification of polypropylene. The mechanism of coke formation on the catalyst was discussed and proposed.

During the catalytic steam gasification process, the catalyst was suggested to be reduced and partially cracked into small particles which might be due to gas reforming reactions inside the catalyst. Layered carbons, consisting of metal carbides or monoatomic carbons or carbonaceous species, was suggested to be formed initially. This is followed by formation of filamentous carbons on the top of the layered carbons with further gasification reactions.

Mg addition into the Ni-Al catalyst was found to increase the reducible NiO phases and the strength of catalyst, thus, resulting in a better performance of the catalyst in terms of hydrogen production. The increase of calcination temperature of the Ni-Mg-Al catalyst was suggested to reduce the catalytic activity and slightly increase the stability of the catalyst.

Acknowledgements

The authors are grateful for the financial support of the Overseas Research Student Award Scheme (UK) and the International Research Studentships Scheme (University of Leeds). The authors also thank Mr. Ed Woodhouse for his technical support, the analytical support from Dr. Jude Onwudili and the FIB/SEM analytic support from Mr. John Harrington.

References

[1] T. Miyazawa, T. Kimura, J. Nishikawa, S. Kado, K. Kunimori, K. Tomishige, Catal. Today 115 (2006) 254.
[2] T. Yamaguchi, K. Yamasaki, O. Yoshida, Y. Kanai, A. Ueno, Y. Kotera, Ind. Eng. Chem. Prod. Res. Dev. 25 (1986) 239.
[3] T. Minowa, F. Zhen, T. Ogi, J. Supercrit. Fluids 13 (1998) 253.
[4] D.L. Trimm, Catal. Today 37 (1997) 233.
[5] C. Wu, P.T. Williams, Appl. Catal. B: Environ. 90 (2009) 147.
[6] C. Wu, P.T. Williams, Energy Fuel 22 (2008) 4125.
[7] S. Czernik, R.J. French, Energy Fuel 20 (2006) 754.
[8] C. Wu, P.T. Williams, Appl. Catal. B: Environ. 87 (2009) 152.
[9] X. Cai, X. Dong, W. Lin, J. Nat. Gas Chem. 17 (2008) 98.
[10] I.N. Buffoni, F. Pompeo, G.F. Santori, N.N. Nichio, Catal. Commun. 10 (2009) 1656.
[11] C. Resini, M.C.H. Delgado, S. Presto, L.J. Alemany, P. Riani, R. Marazaa, G. Ramis, G. Busca, Int. J. Hydrogen Energy 33 (2008) 3728.
[12] J. Sehested, Catal. Today 111 (2006) 103.
[13] J.I. Hayashi, S. Hosokai, N. Sonoyama, Process Saf. Environ. Prot. 84 (2006) 409.
[14] S. Takenaka, E. kato, Y. Tomikubo, K. Otsuka, J. Catal. 219 (2003) 176.
[15] M.A. Ermakova, D.Y. Ermakov, G.G. Kuvshinov, Appl. Catal. A: Gen. 201 (2000) 61.
[16] S. Takenaka, H. Ogihara, I. Yamanaka, K. Otsuka, Appl. Catal. A: Gen. 217 (2001) 101.
[17] K. Tomishige, Y. Chen, K. Fujimoto, J. Catal. 181 (1999) 91.
[18] L. Garcia, A. Benedicto, E. Romeo, M.L. Salvador, J. Arauzo, R. Bilbao, Energy Fuel 16 (2002) 1222.
[19] O. Clause, M. Gazzano, F. Trifiro, A. Vaccari, L. Zatorski, Appl. Catal. 73 (1991) 217.
[20] W. Gac, A. Denis, T. Borowiecki, L. Kępiński, Appl. Catal. A: Gen. 357 (2009) 236.
[21] S. Takenaka, Y. Tomikubo, E. kato, K. Otsuka, Fuel 83 (2004) 47.
[22] B. Louis, R. Vieira, A. Carvalho, J. Amadou, M.J. Ledoux, C. Pham-Huu, Top. Catal. 45 (2007) 75.
[23] A. Sacco, P. Hacker, T.N. Chang, A.T.S. Chiang, J. Catal. 85 (1984) 224.
[24] A.J.H.M. Kock, P.K. Detoks, E. Bolleaard, W. Klop, J.W. Geus, J. Catal. 96 (1985) 468.

[25] J.G. McCarty, H.J. Wise, J. Catal. 57 (1979) 406.
[26] C.H. Bartholomew, Catal. Rev. Sci. Eng. 24 (1982) 67.
[27] D.L. Trimm, Catal. Rev. Sci. Eng. 5 (1972) 1.
[28] J.R. Rostrup-Nielsen, D.L. Trimm, J. Catal. 48 (1977) 155.
[29] S. Natesakhawat, R.B. Watson, X. Wang, U.S. Ozkan, J. Catal. 234 (2005) 496.
[30] J.K. Chinthaginjala, D.B. Thakur, K. Seshan, L. Lefferts, Carbon 46 (2008) 1638.
[31] D.L. Trimm, Catal. Today 49 (1999) 3.
[32] V.C.H. Kroll, H.M. Swaan, C. Mirodatos, J. Catal. 161 (1996) 409.
[33] P. Wang, E. Tanabe, K. Ito, J. Jia, H. Morioka, T. Shishido, K. Takehira, Appl. Catal. A: Gen. 231 (2002) 35.
[34] I.A. Ovsyannikova, G.I. Gold'sdenbery, N.A. Koryabkina, R.A. Shkrabina, Z.R. Ismagilov, Appl. Catal. 55 (1989) 75.
[35] N.A. Koryabkina, Z.R. Ismagilov, R.A. Shkabina, E.M. Moroz, V.A. Ushakov, Appl. Catal. 72 (1991) 63.
[36] D. Swierczynski, S. Libs, C. Courson, A. Kiennemann, Appl. Catal. B: Environ. 74 (2007) 211.
[37] C. Courson, E. Makaga, C. Petit, A. Kiennemann, Catal. Today 63 (2000) 427.
[38] C. Courson, L. Udron, D. Swierczynski, C. Petit, A. Kiennemann, Catal. Today 76 (2002) 75.